

AD-A056 385

SRI INTERNATIONAL MENLO PARK CA

A SEARCH BY RADAR BACKSCATTER, FOR IRREGULARITIES PRODUCED BY T--ETC(U)

FEB 78 W G CHESNUT, G N OETZEL, A MCKINLEY

DNA001-77-C-0267

F/G 4/1

NL

UNCLASSIFIED

DNA-4537F

| OF |  
AD  
A056385



END  
DATE  
FILMED  
9 -78  
DDC



AD A 056385

**LEVEL**

(2)

AD-E300 269

DNA 4537F

**A SEARCH BY RADAR BACKSCATTER,  
FOR IRREGULARITIES PRODUCED BY  
THE LAGOPEDO F-REGION ELECTRON  
DEPLETION RELEASES**

SRI International  
333 Ravenswood Avenue  
Menlo Park, California 94025

February 1978

DDC  
RECEIVED  
JUL 20 1978  
B

Final Report for Period 1 June 1977-31 December 1977

CONTRACT No. DNA 001-77-C-0267

APPROVED FOR PUBLIC RELEASE;  
DISTRIBUTION UNLIMITED.

THIS WORK SPONSORED BY THE DEFENSE NUCLEAR AGENCY  
UNDER RDT&E RMSS CODE B322077462 I25AAXHX63343 H2590D.

Prepared for  
Director  
DEFENSE NUCLEAR AGENCY  
Washington, D. C. 20305

AU NO. \_\_\_\_\_  
DDC FILE COPY

78 06 27 050

Destroy this report when it is no longer  
needed. Do not return to sender.





UNCLASSIFIED

SECURITY CLASSIFICATION OF THIS PAGE (When Data Entered)

REPORT DOCUMENTATION PAGE		READ INSTRUCTIONS BEFORE COMPLETING FORM
1. REPORT NUMBER DNA 4537F	2. GOVT ACCESSION NO.	3. RECIPIENT'S CATALOG NUMBER
4. TITLE (and Subtitle) A SEARCH BY RADAR BACKSCATTER, FOR IRREGULARITIES PRODUCED BY THE LAGOPEDO F-REGION ELECTRON DEPLETION RELEASES,		5. TYPE OF REPORT & PERIOD COVERED Final Report, <del>for public</del> 1 Jun 77-31 Dec 77,
7. AUTHOR(s) Walter G. Chesnut George N. Oetzel Archibald McKinley		6. PERFORMING ORG. REPORT NUMBER SRI Project 6440
9. PERFORMING ORGANIZATION NAME AND ADDRESS SRI International 333 Ravenswood Avenue Menlo Park, California 94025		8. CONTRACT OR GRANT NUMBER(s) DNA 001-77-C-0267
11. CONTROLLING OFFICE NAME AND ADDRESS Director Defense Nuclear Agency Washington, D.C. 20305		10. PROGRAM ELEMENT, PROJECT, TASK AREA & WORK UNIT NUMBERS Subtask I25AAXHX633-43
14. MONITORING AGENCY NAME & ADDRESS (if different from Controlling Office) DNA, SBIE		12. REPORT DATE February 1978
15. DISTRIBUTION STATEMENT (of this Report) Approved for public release; distribution unlimited.		13. NUMBER OF PAGES 28 p.
17. DISTRIBUTION STATEMENT (of the abstract entered in Block 20, if different from Report)		14. SECURITY CLASS (of this report) UNCLASSIFIED
18. SUPPLEMENTARY NOTES This work sponsored by the Defense Nuclear Agency under RDT&E RMSS Code B322077462 I25AAXHX63343 H2590D.		15a. DECLASSIFICATION/DOWNGRADING SCHEDULE
19. KEY WORDS (Continue on reverse side if necessary and identify by block number) Spread-F Gradient-Drift Instability Ionospheric Chemical Releases Underdense Radar Scattering Plasma Radar Scattering Equatorial Spread-F		
20. ABSTRACT (Continue on reverse side if necessary and identify by block number) During early September 1977, the Los Alamos Scientific Laboratory launched two rockets bearing the explosive nitromethane into the F-region over Kauai in the Hawaiian Island chain. The detonation of this material produced a large, generally spherically shaped, reduction in the F-region electron density centered at altitudes between 265 and 285 km. The experiment was called Operation Lagopedo. Some plasma theoreticians had expected that the edges of this electron-depleted region would become unstable by the gradient drift		

DD FORM 1 JAN 73 1473 EDITION OF 1 NOV 65 IS OBSOLETE

UNCLASSIFIED

SECURITY CLASSIFICATION OF THIS PAGE (When Data Entered)

410281

CL

UNCLASSIFIED

SECURITY CLASSIFICATION OF THIS PAGE(When Data Entered)

20. ABSTRACT (Continued)

instability process, leading to the generation of magnetic-field-aligned irregularities similar to those produced in the equatorial ionosphere. The naturally produced equatorial irregularities, called spread-F, are regularly detected by magnetic-field-aligned backscatter radar echoes at HF. Therefore, an attempt was made by SRI International to detect the presence of irregularities in the Lagopedo ionospheric hole by the same HF backscatter means.

This report describes the SRI experimental program. The SRI HF radar was capable of detecting field-aligned irregularities with spatial wavelengths between (approximately) 5 and 10 m (16 MHz to 32 MHz radar frequencies). System sensitivity was a factor of 200 to 800 times more sensitive than equatorial equipment used at comparable frequencies. An additional 20 dB of Doppler processing can be achieved during post-mission data reduction if necessary. The magnetic orthogonality condition was met in the vicinity of the Lagopedo electron depletion regions, yet no field-aligned echoes were observed. Tests in the field certified the system sensitivity and antenna characteristics. We are led to believe that irregularities with wavelengths between 5 and 10 m were very weak if present at all. Some discussion of why this might have been so is presented.

Echoes lasting several seconds following the detonation of the second charge were detected at 20 MHz. No explanation for this observation has been generated.

UNCLASSIFIED

SECURITY CLASSIFICATION OF THIS PAGE(When Data Entered)

# CONTENTS

LIST OF ILLUSTRATIONS . . . . .	2
LIST OF TABLES . . . . .	2
1. INTRODUCTION . . . . .	3
2. BACKGROUND . . . . .	5
2.1 F-Region Chemistry Produced by the Detonation . . . . .	5
2.2 Development of Irregularities by the Gradient- Drift Instability Process . . . . .	7
2.3 Radar Backscatter Detection of Irregularities . . . . .	7
2.4 Summary . . . . .	8
3. EXPERIMENTAL PLAN . . . . .	9
4. PREPARATIONS AND SCHEDULE . . . . .	13
5. RESULTS . . . . .	16
6. CONCLUSIONS AND SUMMARY . . . . .	19

ACCESSION for		
NTIS	Whole Section	<input checked="" type="checkbox"/>
DOC	BRI Section	<input type="checkbox"/>
UNANNOUNCED		<input type="checkbox"/>
JUSTIFICATION		
BY		
DISTRIBUTION/AVAILABILITY CODES		
Dist.	A/AIL. and/or	SPECIAL
A		

## ILLUSTRATIONS

1	Magnetic Geometry of SRI Radar Experiment During LASL-Lagopedo Experiment . . . . .	10
2	Computed Beam Patterns (Relative Gain vs Angle) for SRI Lagopedo Radar System, and Antenna 3-dB Beamwidth vs Frequency . . . . .	14
3	Lagopedo Event DOS High-Explosive Echo. Radar frequency = 20.0 MHz . . . . .	18
4	Reflectivity Coefficient vs Frequency for Gyro- radius-Limited Plasma Gradient . . . . .	20

## TABLES

1	Comparison of System Parameters for the Lagopedo Field-Aligned Radar Backscatter Experiment . . . . .	12
2	SRI Lagopedo Radar Parameters Exclusive of Antenna Characteristics . . . . .	13
3	Characteristics of Lagopedo Experiment . . . . .	17

## 1. INTRODUCTION

During the early part of September 1977, the Los Alamos Scientific Laboratory (LASL) launched into the post-sunset ionosphere, rockets carrying the explosive nitromethane. The detonation of this material in the F-region of the ionosphere led to the production of a region depleted in free electron content--an electron hole.<sup>1\*</sup> The purpose of the releases by LASL was to study ionospheric chemistry.

The center of the electron hole was to be located near the peak density of the predetonation F-layer. Because the neutral winds at this altitude were expected to be rather large, it was believed that the gradient-drift instability would be operative and field-aligned irregularities would develop. It was also believed that this unstable environment was amenable to numerical simulation by digital computer. Therefore, it seemed desirable to perform diagnostic measurements that would detect the presence of these instabilities, or striations resulting from the instability, and measure their properties.

SRI International (formerly the Stanford Research Institute) provided a diagnostic to detect whether the environment actually became unstable. The SRI International diagnostic was a radar search for magnetic-field-aligned scattering from the striations. Striations that are produced by the gradient-drift instability in other environments are regularly detected by this radar means. In particular, equatorial spread-F and auroral-zone F-region irregularities have been detected by HF radars. Thus, the technique has proved itself as a valuable diagnostic.

---

\* References are listed at the end of this report.



This report describes the SRI International radar experiment. Section 2 very briefly outlines the ionospheric/explosive products chemistry that is responsible for producing an ionospheric hole, the ideas surrounding the expected production of irregularities, and the concepts involved in detecting the irregularities by radar backscatter. Section 3 describes the experiment plan including radar/release geometry, rationale behind choice of radar operation frequency, and relates equipment sensitivity to that of equipment used by others to detect F-region irregularities at the equator. Section 4 outlines the program schedule and presents further details concerning the radar operating options. Section 5 describes the actual radar operation and results obtained following the LASL nitromethane detonation. Section 6 summarizes and then discusses theoretical concepts that provide a rationale to explain the negative results of field-aligned scattering detection.



## 2. BACKGROUND

This section presents a brief discussion of the LASL rocket experiment. We also discuss the concepts involved in the development of irregularities and the ionospheric environmental parameters that are thought to be important. The section ends with a discussion of the radar scattering phenomenon.

### 2.1 F-Region Chemistry Produced by the Detonation

The LASL launched two rockets bearing payloads of 88 kg of nitromethane/ammonium nitrate explosive into the peak density of the F-region.<sup>1</sup> The detonation of the explosive at that altitude produced CO<sub>2</sub>, H<sub>2</sub>O, and N<sub>2</sub> as products of high-explosive burn. These products rapidly spread outward from the detonation center and were eventually slowed by collisions with the ambient atmospheric species. These products were expected to then alter the ionospheric chemistry in the detonation region.<sup>2</sup>

The electron density in the F-region is normally maintained by a balance among solar ionization, ultimate conversion of the ions so produced to O<sup>+</sup>, and subsequent disappearance of electrons through a two-step process. The first step is the transfer of the positive charge of the atomic O<sup>+</sup> ions by ion-atom interchange with N<sub>2</sub> to produce NO<sup>+</sup> and N. The molecular ion NO<sup>+</sup> subsequently dissociatively recombines with a free electron. The total time constant for this process is determined primarily by the longer time constant associated with the ion-atom interchange reaction. This time constant is given by the following equation:

$$\tau_{ia} = \frac{1}{k_2 N_2} = 6.8 \cdot 10^3 \text{ s} \quad (1)$$

where

$$k_2 = \text{Rate coefficient} = 7.3 \cdot 10^{-13} \text{ cm}^3 \text{ s}^{-1}$$

$$N_2 = \text{Nitrogen molecule density} = 2 \cdot 10^8 \text{ cm}^{-3} \text{ at } 285 \text{ km.}$$

The time constant for the next step--dissociative recombination of  $\text{NO}^+$ --is given approximately by the following equation:

$$\tau_{\text{dr}} = \frac{1}{2\alpha_d N_e} = \frac{1}{2 \cdot 8 \cdot 10^8 \cdot 4 \cdot 10^5} \cong 16 \text{ s} \quad (2)$$

where  $\alpha_d$  is the dissociative recombination coefficient, and  $N_e$  is the electron density. The direct recombination of electrons with  $\text{O}^+$  is by radiative recombination, which has a time constant on the order of  $10^5 \text{ s}$  and is therefore not very important in the natural ionosphere.

The introduction into the F-region of the complex molecules  $\text{H}_2\text{O}$  and  $\text{CO}_2$  from the detonation provides a more rapid path for the disappearance of ionospheric electrons by speeding up the transfer of the positive charge from  $\text{O}^+$  to a molecule, which is then followed by rapid recombination with free electrons.<sup>2</sup> The ionization potential of both water and carbon dioxide are significantly lower than that of atomic oxygen. Thus charge exchange from the  $\text{O}^+$  to the additive molecules is energetically possible; the rate coefficients are also very large. The time constant for this charge exchange depends on the density of these complex molecules, which density would be estimated by hydrodynamic-type calculations. As an example, if 18 kg of water is uniformly distributed in a sphere 50 km in diameter (approximate estimate), the  $\text{H}_2\text{O}$  density would be about  $10^7 \text{ cm}^{-3}$ . The time constant for  $\text{O}^+$  charge exchange is then

$$\tau_{\text{ce}} = \frac{1}{k_1 N_h} = 47 \text{ s} \quad (3)$$

where

$$k_1 = \text{Rate coefficient} = 2.3 \cdot 10^{-9} \text{ cm}^3 \text{ s}^{-1}$$

$$N_h = \text{Water molecule density} = 10^7 \text{ cm}^{-3}.$$

This time constant is to be compared with the value of 6800 s (2 hours!) produced by the reaction described by Eq. (1). The subsequent dissociative recombination of electrons with  $\text{H}_2\text{O}^+$  proceeds at an even faster rate than with the  $\text{NO}^+$  molecules. Thus, the addition of  $\text{H}_2\text{O}$  and  $\text{CO}_2$  into the F-region is expected to rapidly produce a rather large, local decrease in electron density.

## 2.2 Development of Irregularities by the Gradient-Drift Instability Process

The electron hole, of course, has ion gradients at its edges. At the altitude of release (order of 260 to 280 km) theoretical estimates of the neutral-wind velocity indicate neutral flows towards the east with velocities that range from a low of 40 m/s to as high as 100 m/s. Therefore the side of the electron hole through which the wind enters the hole should be unstable to the gradient-drift instability process. Thus if the electron hole is maintained for a long enough period, ionized striations ought to develop and move into the electron-depleted region. No estimates have been supplied to us by those knowledgeable in these phenomena as to the time that would be required for the ionized irregularities to develop. Based on experience with ionized barium clouds, we have assumed that it will take on the order of 30 minutes for the irregularities to appear. If they develop, then we expect that their presence would be detected by radar backscatter.

## 2.3 Radar Backscatter Detection of Irregularities

The radar backscatter process that is believed responsible for detecting equatorial and auroral spread-F at radar frequencies above the F-region plasma frequency is called field-aligned, underdense backscatter.<sup>3, 4, 5</sup> Two conditions must be met in order that radar energy be

reflected back to the radar receiver. The first condition is that the radar waves must be traveling nearly exactly perpendicular to the earth's magnetic field where the scattering takes place. The second condition that must be met is that spatial fluctuations in electron density whose spatial wavelength is equal to one-half the radar wave length (inside the plasma medium) must be generated by the instability process.

Other factors that play a role in determining whether radar echoes can be observed are as follows: The level of fluctuation in electron density must be sufficiently large; the sensitivity of the radar equipment must be great enough or else the amplitude of the reflected signals will be below the level of detectability; and, finally, Faraday rotation and consequent polarization rotation must be overcome by some means.

The choice of a radar operating frequency for the Lagopedo experiment was based on experience in the equatorial region where field aligned backscatter is regularly used to detect the presence of equatorial spread F. Most equipment used for this purpose operates in the HF and VHF bands from frequencies on the order of 18 MHz to 55 MHz. As will be shown later, the SRI radar was operated at frequencies between 16 and 32 MHz.

#### 2.4 Summary

The release by the LASL of  $H_2O$  and  $CO_2$  into the F-region was expected to produce a depletion of electron density in a spherical region that ought to be on the order of 50 km in diameter. The effects of these molecules on the F-region electron density and ionic chemistry was monitored by a number of experiments in the last stage of the rocket or ground-based in the launch area. Plasma theoreticians have hypothesized that the neutral winds blowing through the windward wall of the electron density hole will cause it to go unstable by the gradient drift instability process. If this process actually occurs, then the striations or irregularities that develop ought to be detectable by field-aligned backscatter of radar signals.

### 3. EXPERIMENTAL PLAN

This section presents the considerations that led to the field site location in Hawaii. Figure 1 is a map of the Hawaiian Islands. The map shows the ultimate location of the radar site at Honuapo on the large island of Hawaii. The LASL rockets were to be launched in a northwesterly direction from the Barking Sands Launch Facility on the west coast of the island of Kauai. We show in the diagram two circles of 60 km in diameter labeled UNO and DOS. These represent the approximate diameter and the locations of the ionospheric holes that were actually produced during the LASL experiments.<sup>1</sup> Since the locations are almost precisely the same as the predictions, we show the actual release locations in this figure.

The radar site at Honuapo was located so that the radar beam line would be exactly perpendicular to the earth's magnetic field near the release points for infinite frequency. The actual ionosphere causes refraction. The predictions for ionospheric density led us to plan for a peak F-region density of  $4 \times 10^5 \text{ el/cm}^3$ . We also show in the figure approximate orthogonality contours at an altitude of 300 km for a peak F-region electron density at 300 km of the predicted  $4 \times 10^5 \text{ el/cm}^3$  for radar frequencies of 22.5 and 30 MHz. These contours are approximate because they depend to a slight degree on the details of the underlying ionosphere that are not available.

The radar site was located on the southeastern side of the island of Hawaii in such a manner that a ridge from Mt. Mauna Loa would limit the radar elevation angles to viewing above  $10^\circ$ . By this procedure, interference caused by F-region propagated sea backscatter that might appear at the same range as the release was reduced. The release altitude was expected to be between 260 and 300 km, which was at an elevation angle on the order of  $20^\circ$  from the radar site at a slant range of 650 km.



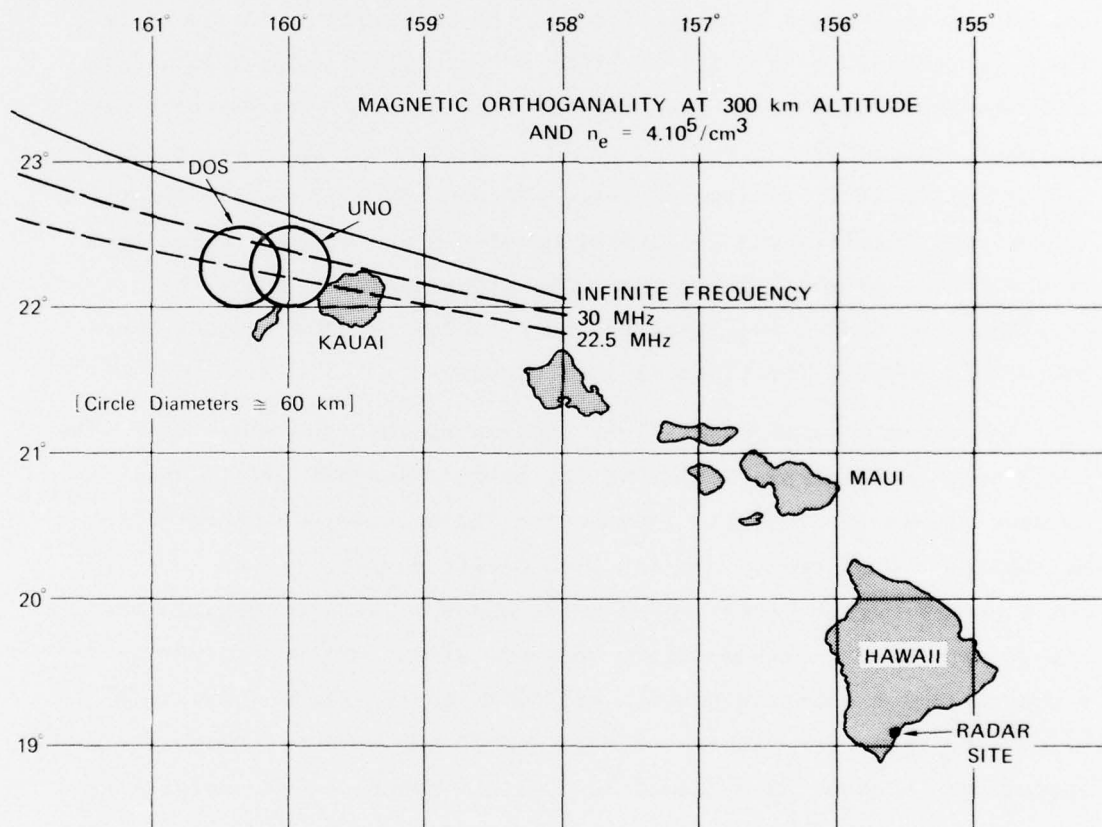


FIGURE 1 MAGNETIC GEOMETRY OF SRI RADAR EXPERIMENT DURING LASL-LAGOPEDO EXPERIMENT



The equipment parameters were chosen by comparing the sensitivity of radar systems used to detect equatorial spread-F with radar equipment available at SRI. Table 1 presents equipment descriptions of three experiments used at the equator. The point-target figure of merit relative to Clemesha's experiment summarizes the comparative system sensitivities.

The one outstanding feature of these data are that Clemesha, working at 18 MHz, was able to use a very insensitive radar and yet detect very strong spread-F signals. At the other frequency extreme, Balsley et al., operating at 55 MHz, found it necessary to use a system with sensitivity on the order of 1000 times as great. They also used Doppler processing that gave significant additional sensitivity. It was apparent, therefore, that the underdense backscatter from F-region irregularities has a very steep frequency dependence. Thus, lower frequencies were preferred because of the apparently larger cross sections produced by the medium.

The radar parameters used by SRI are shown in the last column. The radar was modified to be operated alternately at two frequencies between 16 and 32 MHz. During this modification work, it was also found that the radar could be modified to operate sequentially at all 40 of its frequencies. Equipment was so modified to operate with 128 pulses per frequency in a phase-coherent manner. In this way an additional 20 dB of sensitivity can be achieved through Doppler processing. Multiple frequencies also mitigate loss of return because of Faraday rotation, and also provide protection against interference from nearby radio transmitters.

The bottom line presents the relative single-pulse, point-target sensitivity of each of the four radars described. The table shows that the SRI equipment was from 200 to 800 times more sensitive than radars used at the equator at comparable frequencies. Through Doppler processing, an additional multiplying factor of 100 (20 dB) can be achieved.

Table 1

COMPARISON OF SYSTEM PARAMETERS FOR THE  
LAGOPEDO FIELD-ALIGNED RADAR BACKSCATTER EXPERIMENT

	SYSTEMS USED TO DETECT AND STUDY EQUATORIAL F-REGION IRREGULARITIES			LAGOPEDO
INVESTIGATOR	CLEMESHA <sup>3</sup>	KELLEHER SKINNER <sup>4</sup>	BALSLEY HAERENDEL GREENWALD <sup>5</sup>	SRI INTERNATIONAL
LOCATION	LEGON, GHANA	NAIROBI, KENYA	THUMBA, INDIA	HANUAPO, HAWAII
FREQUENCY (MHz)	18	27.8	55	16-32
PEAK POWER (kW)	1.0	2.0	8.0	30.0
PULSE LENGTH ( $\mu$ s)	300	1000	50-200	250
ANTENNA DESCRIPTION	3 ELEMENT YAGI	6 DIPOLES AND 5 ELEMENT YAGI	208 DIPOLES WITH REFLECTORS	4 LOG PERIODICS
ANTENNA GAIN (dB)	< 10	~11 <12	~27	~17
POINT TARGET FIGURE OF MERIT ( $P_T G^2 \lambda \tau$ )	1.0	1.33	360, 1435	198, 794

#### 4. PREPARATIONS AND SCHEDULE

Work was initiated on refurbishing the radar equipment, radar van, and computer equipment in early June 1977. Antenna design and pattern calculations were performed during the same period and led to the choice of four ganged log-periodic antennas. Figure 2 shows horizontal antenna patterns at the extreme frequencies used in this experiment. The choice of these beamwidths seemed adequate to cover anticipated motion of the ionospheric hole. Table 2 presents a summary of radar operating options.

Table 2

##### SRI LAGOPEDO RADAR PARAMETERS EXCLUSIVE OF ANTENNA CHARACTERISTICS

###### Receiver

Frequency coverage: 2-32 MHz

Receiver bandwidth: 16 kHz and 4 kHz

10 kHz and 500 kHz video out (phase coherent)

###### Transmitter

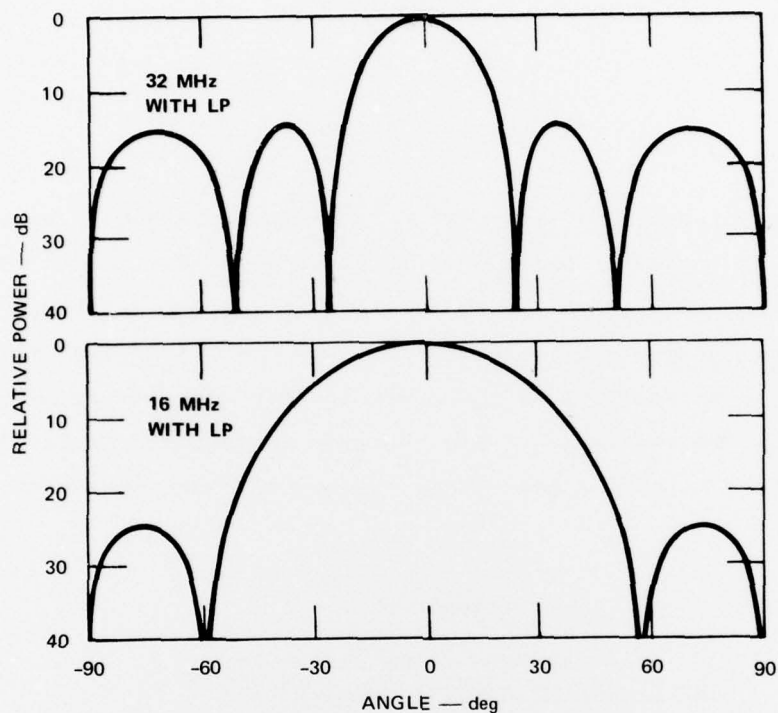
Transmitter power: 30 kW peak pulse

Maximum duty at rated output: 0.02 (2%)

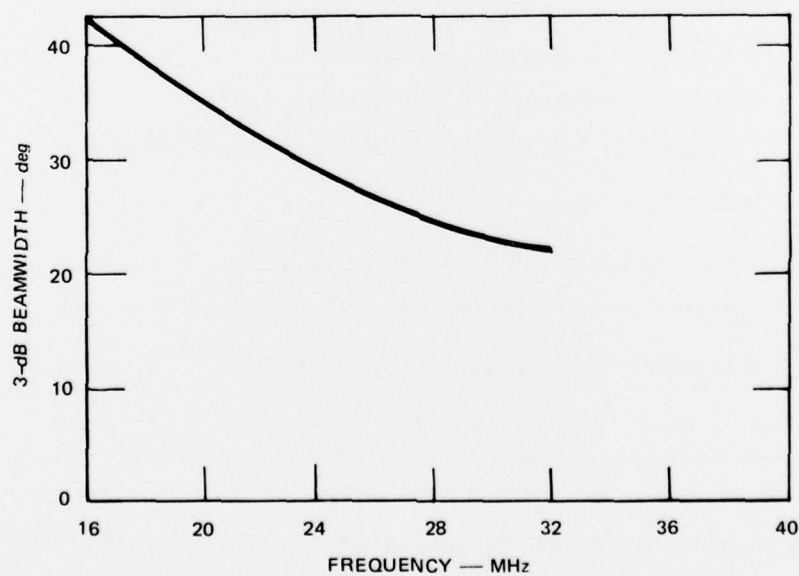
Pulsewidth: 50, 100, 200, 500, 100  $\mu$ s

PRF: 2, 5, 10, 20, 50, 100 per second

Equipment was shipped by Matson Lines to Hilo, Hawaii on 12 August, arriving in Hilo on 17 August. The radar was installed at the Honuapo field site and was operational for the first Lagopedo release on the



(a) COMPUTED HORIZONTAL BEAM PATTERN FOR 16 MHz AND 32 MHz



(b) ANTENNA 3-dB AZIMUTHAL BEAMWIDTH vs FREQUENCY

FIGURE 2 COMPUTED BEAM PATTERNS (relative gain vs angle) FOR SRI LAGOPEDO RADAR SYSTEM, AND ANTENNA 3-dB BEAMWIDTH vs FREQUENCY

evening of 1 September (Hawaiian time). During the period between installation and equipment tear-down on 12 September (Hawaiian time), studies were also made of meteor backscatter echoes, and sea backscatter echoes propagated via the F-region. These studies were performed to confirm that the antenna beam characteristics, including the effects of the mountain as a clutter fence, were consistent with our theoretical expectations.

Equipment was returned via Matson Lines to SRI during the middle of September 1977.



## 5. RESULTS

Table 3 presents the statistics regarding the Lagopedo actual releases UNO and DOS. On event Lagopedo UNO, no effects of the detonation were observed by the radar. The equipment was operated for one hour after release, searching for field-line irregularities. No irregularities were observed in real time by radar operators nor in range-time-intensity (RTI) records produced back at SRI. Data were recorded digitally on magnetic tape so that, should it be of interest, a further search may be made using Doppler processing for an additional 20 dB of signal sensitivity.

On event DOS, the radar was operated for several minutes before and after anticipated release time at a fixed frequency of 20 MHz. This frequency was chosen because it was free of propagated interference. The detonation led to an environment that was detected as a radar echo. Figure 3 presents an RTI plot that shows this echo. The explosion echo is seen as the darkened region at a virtual slant range of 720 km at 0604:10 UT.

Though the NOAA digisonde located at Kauai detected weak spread F throughout the evening not associated with the release, no naturally produced field-aligned echoes were detected by the SRI radar. The radar was operated for an hour after release. No release-associated field-aligned echoes were observed to develop during this operating period.



Table 3

## CHARACTERISTICS OF LAGOPEDO EXPERIMENT

	Event UNO	Event DOS
<u>SRI Radar Location</u>		
Latitude ( $^{\circ}$ N)	19.092	19.092
Longitude ( $^{\circ}$ W)	155.55	155.55
<u>Release Parameters (Ref. 1)</u>		
Event time (UT)	0554:00 9/2/77	0604:10 9/12/77
Event time (HT)	1954:00 9/1/77	2004:10 9/11/77
Event altitude (km)	261.22	282.86
Event latitude ( $^{\circ}$ N)	22.279	22.262
Event longitude ( $^{\circ}$ W)	159.982	160.351
Released in sunlight	Yes	No
<u>Release Geometry Relative to SRI Radar</u>		
Azimuth (deg)	308.3	306.0
Elevation (deg)	21.13	20.0
Slant range (km)	648.0	675.9
Great circle distance (km)	581.4	611.2
<u>Ionospheric Parameters (Ref. 1)</u>		
Peak electron density ( $\text{el}/\text{cm}^3$ )	$1.0 \times 10^6$	$3.4 \times 10^5$
Height of peak (km)	275	323
F2 layer scale height (km)	42	65
Stability	Stable	Weak spread-F

12 SEPTEMBER 1977

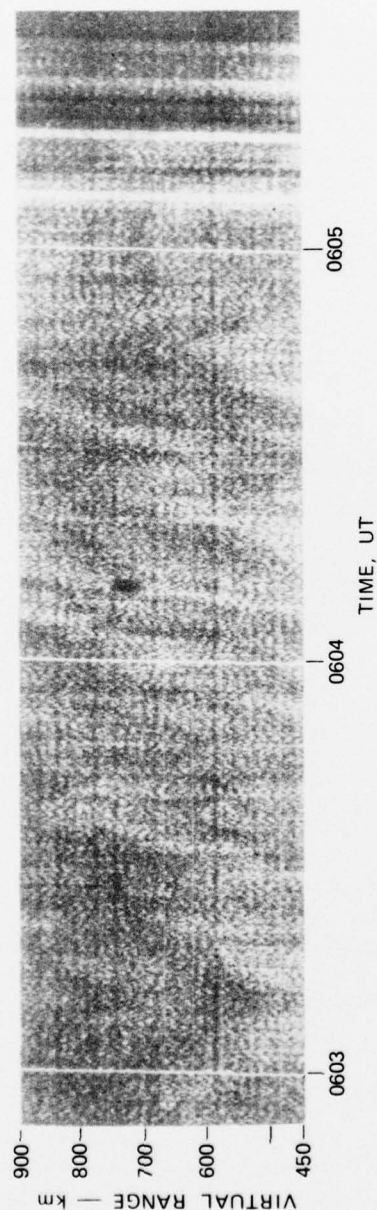


FIGURE 3 LAGOPEDO EVENT DOS HIGH-EXPLOSIVE ECHO. Radar frequency = 20.0 MHz.

## 6. CONCLUSIONS AND SUMMARY

Radar equipment to detect magnetic-field-aligned irregularities that might have grown on the edges of the hole were installed and made operational in time for the first LASL Lagopedo release. Tests on meteor backscatter, F-region-propagated sea backscatter, and standard radar calibrating procedures showed that the equipment sensitivity, including antenna characteristics, were as planned.

During the Lagopedo release experiments, the radar was operated in a step-frequency mode from 16 through 32 MHz, 128 pulses per frequency, and a pulsewidth of 200  $\mu$ s at a PRF of 50 or 100 Hz during the search for field-aligned echoes. The releases took place in locations very close to those used in planning the experiment. Therefore, we have every reason to believe that the magnetic orthogonality condition was met at some radar frequencies at some places in the cloud throughout the entire one-hour observing period following detonation. We conclude that if irregularities did form on the side of the Lagopedo electron depletion region, then the gradients in electron density were sufficiently gradual that the radar reflectivity was below our detectability.

In planning for this experiment, some theoretical studies were performed to attempt to explain why equatorial F-region irregularities were so very easily detected at 18 and 28 MHz but were, by comparison, very weak at 55 MHz. Based on studies of barium clouds as well as in-situ measurements in equatorial spread-F, we are of the opinion that the field-aligned echoes are produced by reflections off the gradients (edges) of the irregularity structures.

We assume that in a very dynamically unstable environment, the steepest ion gradient that can develop is that determined by the gyro-radius distribution for oxygen ions. Figure 4 shows the results of calculations of the reflectivity coefficient versus frequency for this

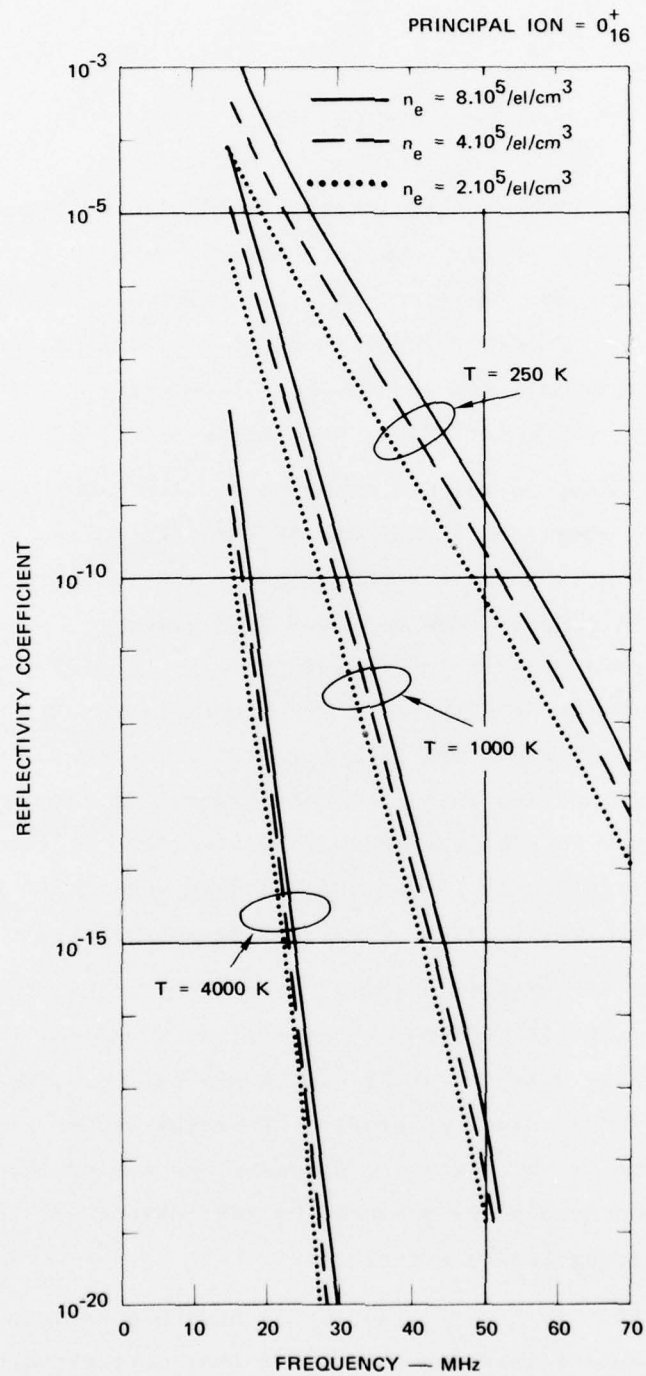


FIGURE 4 REFLECTIVITY COEFFICIENT vs FREQUENCY FOR GYRORADIUS-LIMITED PLASMA GRADIENT

type of gradient. The calculations were performed for three different ionospheric temperatures, and for three values of electron density at each temperature. These data show an extremely steep frequency dependence that is needed to explain the character of the various types of instrumentation required for detection of equatorial spread-F as outlined in Table 1.

The data in Figure 4 may also be viewed as providing the reflectivity coefficient for a plasmic gradient with gradient distances of 1.25 m (curves labeled  $T = 250$  K), 2.5 m (curves labeled  $T = 1000$  K), and 5 m (curves labeled  $T = 4000$  K). Viewed in this light, if irregularities do form but are not extremely dynamic, then the gradient at irregularity edges would be spread by diffusion so that the gradient would be more gradual than the limiting value produced by the gyroradius distribution. Thus, if the weak, naturally produced spread-F that was detected by the NOAA digisonde but not by the SRI radar was due to irregularities similar in character to equatorial spread-F, then we would have to conclude that the irregularity environment was weak so that the steep gradients needed for underdense scattering at the SRI radar frequencies were not produced.

The NOAA digisonde detected both of the electron depletion regions by multiple reflection paths inside the holes. The digisonde data do not give any indication that the electron depletion regions produced field-aligned irregularities; however, it was not anticipated that the instrument would indicate the presence of such irregularities. The SRI radar detected no field-aligned irregularities associated with the release. We conclude that probably no irregularities formed, but if they did, on the basis of the concepts that led to the data in Figure 4, the gradients on the edges of striations were more shallow than those associated with the dynamic situation found in the equatorial region.



#### REFERENCES

1. M. B. Pongratz, G. M. Smith, C. D. Sutherland, and J. Zinn, "Lagopedo--Two F-Region Ionospheric Depletion Experiments," preprint of article, University of California, Los Alamos Scientific Laboratory, Los Alamos, NM (December 1977).
2. P. A. Bernhardt, "The Response of the Ionosphere to the Injection of Chemically Reactive Vapors," Technical Report 17, SEL-76-009, Stanford Electronics Laboratories, Radioscience Laboratory, Stanford University, Stanford, CA (May 1976).
3. B. R. Clemesha, "An Investigation of the Irregularities in the F-Region Associated with Equatorial Type Spread-F," J. Atmos. Terr. Phys., Vol. 26, pp. 91 to 112 (1964).
4. R. F. Kelleher and N. J. Skinner, "Studies of F Region Irregularities at Nairobi II--By Direct Backscatter at 27.8 MHz," Ann. Geophys., t. 27, fasc. 2, p. 195 a 200 (1971).
5. B. B. Balsley, G. Haerendel, and R. A. Greenwald, "Equatorial Spread F: Recent Observations and a New Interpretation," J. Geophys. Res., Vol. 77, No. 28, p. 5625-5628 (October 1972).



## DISTRIBUTION LIST

### DEPARTMENT OF DEFENSE

Assistant Secretary of Defense  
Cmd, Cont., Comm. & Intell.  
ATTN: M. Epstein  
ATTN: J. Babcock

Assistant to the Secretary of Defense  
Atomic Energy  
ATTN: ATSD (AE)

Director  
Command and Control Technical Center  
ATTN: C-312, R. Mason  
ATTN: C-650, G. Jones  
ATTN: C-650  
ATTN: C-650, W. Heidig

Director  
Defense Advanced Rsch. Proj. Agency  
ATTN: Nuclear Monitoring Research  
ATTN: Strategic Tech. Office

Defense Communication Engineer Center  
ATTN: Code R410, J. McLean

Director  
Defense Communications Agency  
ATTN: Code 480  
ATTN: Code 810, R. Rostron  
ATTN: Code 101B  
ATTN: Code R103, M. Raffensperger

Defense Communications Agency  
WWMCCS System Engineering Org.  
ATTN: R. Crawford

Defense Documentation Center  
Cameron Station  
12 cy ATTN: TC

Director  
Defense Nuclear Agency  
ATTN: TISI  
ATTN: STVL  
ATTN: DDST  
3 cy ATTN: TITL  
8 cy ATTN: RAAE

Commander, Field Command  
Defense Nuclear Agency  
ATTN: FCPR

Director  
Joint Strat. Tgt. Planning Staff  
ATTN: JLTW-2

Chief  
Livermore Division, Field Command, DNA  
Lawrence Livermore Laboratory  
ATTN: FCPL

Director  
National Security Agency  
ATTN: W14, P. Clark  
ATTN: R5  
ATTN: R52, J. Skillman

### DEPARTMENT OF DEFENSE (Continued)

OJCS/J-3  
ATTN: WWMCCS, Eval. Ofc., Mr. Toma  
  
Under Secretary of Defense for Rsch. & Engrg.  
ATTN: S&SS (OS)

### DEPARTMENT OF THE ARMY

Commander/Director  
Atmospheric Sciences Laboratory  
U.S. Army Electronics Command  
ATTN: DRSEL-BL-SY-A, F. Niles

Chief C-E Services Division  
U.S. Army Communications Cmd.  
ATTN: CC-OPS-CE

Commander  
Harry Diamond Laboratories  
ATTN: DELHD-NP, F. Wimenitz  
ATTN: DELHD-NP  
ATTN: DELHD-TT, M. Weiner

Commander  
U.S. Army Foreign Science & Tech. Ctr.  
ATTN: P. Crowley

Commander  
U.S. Army Nuclear & Chemical Agency  
ATTN: Library

Commander  
U.S. Army SATCOM Agency  
ATTN: Doc. Con.

### DEPARTMENT OF THE NAVY

Chief of Naval Research  
ATTN: Code 461

Commander  
Naval Electronics Systems Command  
Naval Electronics Systems Cmd. Hqs.  
ATTN: PME 117  
ATTN: PME 117-T, Satellite Comm. Proj. Off.

Commander  
Naval Ocean Systems Center  
ATTN: Code 2200

Director  
Naval Research Laboratory  
ATTN: Code 7700, T. Coffey  
ATTN: Code 5465, Prop. Applications  
ATTN: Code 5460, Electromag Prop. Br.  
ATTN: Code 7701, J. Brown  
ATTN: Code 5430, Satellite Comm.  
ATTN: Code 5400, B. Wald

Officer-in-Charge  
Naval Surface Weapons Center  
ATTN: Code WA501, Navy Nuc. Prgms. Off.

DEPARTMENT OF THE NAVY (Continued)

Commander  
Naval Surface Weapons Center  
Dahlgren Laboratory  
ATTN: DF-14, R. Butler

Director  
Strategic Systems Project Office  
ATTN: NSSP-2722, F. Wimberly  
ATTN: NSP-2141

DEPARTMENT OF THE AIR FORCE

AF Geophysics Laboratory, AFSC  
ATTN: OPR-1, J. Ulwick  
ATTN: PHD, J. Mullen  
ATTN: SUOL, Rsch. Lib.  
ATTN: PHP, J. Aarons  
ATTN: PHD, J. Buchau

AF Weapons Laboratory, AFSC  
ATTN: SUL  
ATTN: DYC, J. Kamm

AFTAC  
ATTN: TN

Air Force Avionics Laboratory, AFSC  
ATTN: AAD, A. Johnson

Commander  
Foreign Technology Division, AFSC  
ATTN: NICD Library

Commander  
Rome Air Development Center, AFSC  
ATTN: EMTLD, Doc. Lib.

Commander  
Rome Air Development Center, AFSC  
ATTN: EEP

DEPARTMENT OF ENERGY

University of California  
Lawrence Livermore Laboratory  
ATTN: Tech. Info., Dept. L-3

Los Alamos Scientific Laboratory  
ATTN: Doc. Con. for P. Keaton  
ATTN: Doc. Con. for J. Wolcott  
ATTN: Doc. Con. for R. Jefferies  
ATTN: Doc. Con. for J. Zinn  
ATTN: Doc. Con. for R. Taschek

Sandia Laboratories  
ATTN: Doc. Con. for Org. 1353, W. Brown  
ATTN: Doc. Con. for Org. 1732, J. Martin  
ATTN: Doc. Con. for Org. 1722, D. Dahlgren

OTHER GOVERNMENT AGENCIES

Institute for Telecommunications Sciences  
National Telecommunications & Info. Admin.  
ATTN: W. Utlaut

National Oceanic & Atmospheric Admin.  
Environmental Research Laboratories  
ATTN: C. Rufenach

DEPARTMENT OF DEFENSE CONTRACTORS

Aerospace Corporation  
ATTN: I. Garfunkel  
ATTN: T. Salmi  
ATTN: N. Stockwell  
ATTN: SMFA for PWV  
ATTN: J. Carter

University of California at San Diego  
ATTN: H. Booker

COMSAT Laboratories  
ATTN: R. Tour

Cornell University  
Department of Electrical Engineering  
ATTN: D. Farley, Jr.

ESL, Inc.  
ATTN: C. Prettie  
ATTN: J. Marshall

Ford Aerospace & Communications Corp.  
ATTN: J. Mattingley

General Electric Company  
TEMPO-Center for Advanced Studies  
ATTN: W. Knapp  
ATTN: DASIAC

General Electric Company  
ATTN: F. Reibert

General Research Corporation  
Santa Barbara Division  
ATTN: J. Garbarino  
ATTN: J. Ise, Jr.

Geophysical Institute  
University of Alaska  
ATTN: Tech. Lib.

GTE Sylvania, Inc.  
Electronics Systems Grp-Eastern Div.  
ATTN: M. Cross

University of Illinois  
Department of Electrical Engineering  
ATTN: K. Yeh

Institute for Defense Analyses  
ATTN: E. Bauer

Intl. Tel. & Telegraph Corporation  
ATTN: Tech. Lib.

Jaycor  
ATTN: S. Goldman

Johns Hopkins University  
Applied Physics Laboratory  
ATTN: Document Librarian  
ATTN: T. Potemra  
ATTN: J. Dassoulas

MIT Lincoln Laboratory  
ATTN: Lib. A-082 for D. Towle

DEPARTMENT OF DEFENSE CONTRACTORS (Continued)

McDonnell Douglas Corporation  
ATTN: Tech. Library Services

Mission Research Corporation  
ATTN: D. Sowle  
ATTN: R. Hendrick  
ATTN: F. Fajen  
ATTN: R. Bogusch

The MITRE Corporation  
ATTN: Chief Scientist, W. Sen

Physical Dynamics, Inc.  
ATTN: J. Workman

Physical Dynamics, Inc.  
ATTN: F. Fremouw

R&D Associates  
ATTN: W. Karzas  
ATTN: B. Gabbard  
ATTN: R. Lelevier

DEPARTMENT OF DEFENSE CONTRACTORS (Continued)

Raytheon Company  
ATTN: B. Adams

Science Applications, Inc.  
ATTN: D. Hamlin  
ATTN: D. Sachs  
ATTN: L. Linson

SRI International  
ATTN: W. Chesnut  
ATTN: G. Oetzel  
ATTN: A. McKinley  
ATTN: D. McDaniel  
ATTN: R. Halce  
ATTN: V. Gonzales  
ATTN: C. Rino  
ATTN: W. Jaye  
ATTN: R. Leadabrand

The Rand Corporation  
ATTN: C. Crain  
ATTN: E. Bedrozian